Large-Scale Characteristics of Rapidly Intensifying Tropical Cyclones in the North Atlantic Basin

JOHN KAPLAN

Hurricane Research Division, NOAA/AOML, Miami, Florida

MARK DEMARIA

Regional and Mesoscale Meteorology Team, NOAA/NESDIS, Fort Collins, Colorado

(Manuscript received 17 December 2002, in final form 26 April 2003)

ABSTRACT

The National Hurricane Center (NHC) and Statistical Hurricane Intensity Prediction Scheme (SHIPS) databases are employed to examine the large-scale characteristics of rapidly intensifying Atlantic basin tropical cyclones. In this study, rapid intensification (RI) is defined as approximately the 95th percentile of over-water 24-h intensity changes of Atlantic basin tropical cyclones that developed from 1989 to 2000. This equates to a maximum sustained surface wind speed increase of 15.4 m s^{-1} (30 kt) over a 24-h period. It is shown that 31% of all tropical cyclones, 60% of all hurricanes, 83% of all major hurricanes, and all category 4 and 5 hurricanes underwent RI at least once during their lifetimes.

The mean initial ($t = 0$ h) conditions of cases that undergo RI are compared to those of the non-RI cases. These comparisons show that the RI cases form farther south and west and have a more westward component of motion than the non-RI cases. In addition, the RI cases are typically intensifying at a faster rate during the previous 12 h than the non-RI cases. The statistical analysis also shows that the RI cases are further from their maximum potential intensity and form in regions with warmer SSTs and higher lower-tropospheric relative humidity than the non-RI cases. The RI cases are also embedded in regions where the upper-level flow is more easterly and the vertical shear and upper-level forcing from troughs or cold lows is weaker than is observed for the non-RI cases. Finally, the RI cases tend to move with the flow within a higher layer of the atmosphere than the non-RI cases.

A simple technique for estimating the probability of RI is described. Estimates of the probability of RI are determined using the predictors for which statistically significant differences are found between the RI and non-RI cases. Estimates of the probability of RI are also determined by combining the five predictors that had the highest individual probabilities of RI. The probability of RI increases from 1% to 41% when the total number of thresholds satisfied increases from zero to five. This simple technique was used in real time for the first time during the 2001 Atlantic hurricane season as part of the Joint Hurricane Testbed (JHT).

1. Introduction

An analysis of recent Atlantic basin tropical cyclone (TC) forecasts conducted by DeMaria et al. (2002) shows that the official National Hurricane Center (NHC) TC intensity forecasts are now skillful out to 72 h. However, that same study also indicated that the official NHC intensity forecasts are much less skillful than the official NHC track forecasts. This finding is consistent with the results of Gross (2001) that show that operational forecast models are substantially more skillful in predicting a tropical cyclone's track than its intensity. While the forecasting of TC intensity change in general has been quite difficult, the forecasting of rapid intensification (RI) has been particularly challenging as was illustrated by the unanticipated RI that occurred during recent Hurricanes Opal (1995) and Bret (1999). Both Opal (Lawrence et al. 1998) and Bret (Lawrence et al. 2001) intensified rapidly and became category 4 hurricanes on the Saffir–Simpson hurricane scale (Saffir 1973; Simpson 1974) within 48 h of U.S. landfall. Fortunately, both of these storms weakened substantially after undergoing RI and made landfall as minimal category 3 hurricanes. Nevertheless, these two systems produced an estimated $3 billion in damage and claimed nine lives even though Bret made landfall in a sparsely populated region of Texas. Clearly, the unexpected RI of these hurricanes so close to the coast underscores the need for improving our understanding of TC intensification, especially the RI process.

The inability to forecast RI is consistent with our limited understanding of TC intensity change in general.

Corresponding author address: John Kaplan, Hurricane Research Division, NOAA/AOML/4301 Rickenbacker Cswy., Miami, FL 33149.
E-mail: john.kaplan@noaa.gov

In the past, researchers have typically examined the role that the ocean, inner-core processes, and environmental interactions play in tropical cyclone intensity change. Although some intensity change studies have examined the importance of all three of these effects, most have focused on only one of these three areas. In some instances, these studies have discussed possible physical mechanisms for RI; however, very few studies have been devoted solely to this topic. Consequently, many questions remain concerning the precise physical mechanisms that are responsible for RI. The results of some notable TC intensity change studies are discussed below with emphasis placed upon their relevance to RI.

The fundamental impact of the ocean on TC intensity has been stressed for many years (Byers 1944; Miller 1958; Malkus and Riehl 1960). For the most part, these early studies tended to focus solely on the beneficial aspects of the ocean on TC intensity. More recently, observational (Black 1983) and modeling studies (Sutyrin and Khain 1979; Bender et al. 1993; Bender and Ginis 2000) have shown that upwelling and vertical mixing of the cool underlying ocean by the TC vortex can produce a negative feedback between the atmosphere and ocean. However, Shay et al. (2000) suggest that warm ocean eddies may reduce the magnitude of the mixing of subsurface water, thereby decreasing the magnitude of this negative feedback. They examined the impact of a Gulf of Mexico eddy on the intensity of Hurricane Opal and concluded that the eddy may have contributed to Opal's RI. The numerical modeling results of Hong et al. (2000) also support the importance of the Gulf of Mexico eddy on Opal's rate of intensification. They employed the Naval Research Laboratory's Coupled Ocean–Atmosphere Mesoscale Prediction System (COAMPS) to simulate the effect of the eddy on Opal's intensity. Their results suggest that the Gulf eddy may have lowered Opal's central pressure by an additional 10 hPa.

The importance of inner-core processes on tropical cyclone intensity change has been the subject of both observational and theoretical studies. One inner-core process that has been linked to changes in TC intensity is concentric eyewall cycles. As noted in Willoughby et al. (1982), concentric eyewalls are characterized by the development of a secondary ring of convection around an existing inner eyewall. This secondary (outer) eyewall may contract and replace the inner eyewall, sometimes resulting in marked changes in TC intensity. Willoughby et al. (1982) used National Oceanic and Atmospheric Administration (NOAA) WP-3D flight-level data to examine the effect of both the formation and dissipation of a tropical cyclone's inner and outer eyewall on TC intensity. Their results suggest that the collapse of an inner eyewall can result in significant TC weakening. However, they also showed that contraction of an outer eyewall can produce a period of substantial TC intensification. The theoretical results of Montgomery and Kallenbach (1997) suggest that a TC vortex can intensify as a result of the axisymmetrization of a convectively induced localized region of positive potential vorticity (PV). When this localized region of positive PV is introduced near the radius of maximum wind (RMW), an increase in the eyewall tangential winds can result. However, when a region of positive PV is generated at a sufficient distance outside the RMW, the main impact is for the tangential winds beyond the eyewall to increase while those near the eyewall remain relatively unchanged (Moller and Montgomery 2000). Moller and Montgomery (2000) speculated that this outer wind maximum may contract, a process that Willoughby et al. (1982) has shown can result in large rates of TC intensification.

Previous studies have shown that vertical shear plays a significant role in modulating TC intensity. Gray (1968) showed that storm development is associated with low vertical wind shear, while Merrill (1988) showed that intensifying hurricanes tended to have lower vertical shear than nonintensifying hurricanes. These earlier studies led DeMaria and Kaplan (1994a) to evaluate the feasibility of employing vertical shear as a predictor in the Statistical Hurricane Intensity Prediction Scheme (SHIPS). Their results showed that vertical shear was the second-most important predictor (after the oceanic predictors) in the SHIPS model. More recently, Frank and Ritchie (1999, 2001) have employed the fifth-generation Pennsylvania State University–National Center for Atmospheric Research (Penn State–NCAR) Mesoscale Model (MM5) to study the impact of vertical shear on TC intensity. Their results indicate that low (high) shear can result in rapid intensification (filling) of the TC vortex. Finally, the analytical results of DeMaria (1996) indicate that storm size, intensity, and latitude can modulate the relationship between vertical shear and TC intensity.

Pfeffer (1958) and Pfeffer and Challa (1981) have discussed the importance of external forcing from upper-level troughs on TC intensity change. More recently, Molinari and coauthors (Molinari and Vollaro 1989, 1990; Molinari et al. 1995) examined the role of an upper-level trough in the intensification of Hurricane Elena (1985), and offered two possible mechanisms for TC intensification associated with hurricane–trough interactions. In their second study, Molinari and Vollaro (1990) solved the Eliassen balanced vortex equation to show that the interaction between Elena and the upper-level trough resulted in an enhancement of Elena's radial-vertical circulation. They speculated that this process may have triggered the formation and contraction of a secondary eyewall and ultimately the rapid pressure falls observed in Elena. Alternatively, Molinari et al. (1995) hypothesized that the superposition of an upper-level positive PV anomaly above Hurricane Elena may have initiated the wind-induced surface heat exchange (WISHE) mechanism (Emanuel 1986), and they speculated that the initiation of the WISHE mechanism may have led to the rapid pressure falls observed in Elena

TABLE 1. The definitions of the climatological and persistence and synoptic variables. The synoptic variables are shown in boldface. Those variables not employed in the SHIPS model are underlined. The units of each variable are also shown.

Variable	Units	Definition
VMX	m s^{-1}	Maximum sustained surface wind speed
LAT	°N	Latitude
LON	°W	Longitude
SPD	m s^{-1}	Storm speed of motion
DVMX	m s^{-1}	Intensity change during the previous 12 h
USTM	m s^{-1}	u component of storm motion
JDAY		Absolute value of (Julian date - 253)
SST	°C	Sea surface temperature
POT	m s^{-1}	Maximum potential intensity (MPI) - VMX
SHR	m s^{-1}	850–200-hPa vertical shear averaged from r = 200–800 km
U200	m s^{-1}	200-hPa u component of wind averaged from r = 200–800 km
T200	°C	200-hPa temperature averaged from r = 200–800 km
RHLO	%	850–700-hPa relative humidity averaged from r = 200–800 km
Z850	10^{-7} s^{-1}	850-hPa relative vorticity averaged for $r \leq 1000$ km
REFC	m s^{-1} day^{-1}	200-hPa relative eddy angular momentum flux convergence averaged from r = 100–600 km
SLYR	hPa	Pressure of the center of mass of layer for which the environmental winds best match the current storm motion averaged from r = 200–800 km

(1985). While the above studies suggest that the interaction of an upper-level trough and a tropical cyclone might result in rapid deepening, the observational results of Hanley et al. (2001) suggest that a tropical cyclone is much less likely to strengthen rapidly when experiencing strong external forcing from an upper-level trough or cold low than when located in a relatively undisturbed environment. The modeling results of Frank and Ritchie (1999) and Emanuel (2000) also indicate that rapid intensification can occur without external forcing from upper-level troughs or cold lows.

In addition to the above studies, a few others have focused more explicitly on RI. Holliday and Thompson (1979) examined the climatological characteristics of rapidly intensifying northwest Pacific typhoons. They found that a sufficiently deep layer of warm water was necessary for RI, and that RI was more prevalent during the night and for TCs with smaller than average eye diameters. During the development of SHIPS, DeMaria and Kaplan (1994a) performed a statistical analysis of the 1989–92 cases that exhibited the largest 48-h intensification rates. Their results showed that these cases were smaller than average, were in an environment with low vertical shear and weak upper-level forcing, and were further from their empirically derived maximum potential intensity and were intensifying faster than the sample mean. More recently, Bosart et al. (2000) examined the episode of RI that occurred in Opal (1995). They concluded that Opal's RI was due to a combination of several factors: enhanced divergence in the equatorward side of the entrance region of an upper-level jet, low vertical shear, and enhanced heat and moisture fluxes that resulted when Opal traversed a warm Gulf eddy.

The goal of this study is to determine if the RI mechanisms proposed in previous studies can be confirmed for a large dataset. To satisfy this goal, the NHC HURDAT file (Jarvinen et al. 1984) and the SHIPS (DeMaria and Kaplan 1999, hereafter DK99) database are used to examine the environmental conditions that appear to be favorable for RI. The conditions that are present for cases that underwent RI are evaluated to determine if they are significantly different from those that existed for cases with less rapid intensification rates. The dataset used in this study is described in section 2. A statistical analysis of Atlantic basin 24-h intensity changes is provided in section 3. A comparison of the conditions present at the start of each period of RI to those that existed for all of the remaining 24-h time periods is presented in section 4. Finally, some concluding remarks are offered in section 5.

2. Data and analysis

The database for this study consists of all Atlantic basin TCs (including nondeveloping depressions) that developed from 1989 to 2000. Table 1 shows the climatological and persistence, and large-scale variables that were evaluated for each TC. These variables were determined from the NHC HURDAT file (Jarvinen et al. 1984) and the SHIPS (DK99) database. The HURDAT file consists of 6-h estimates of position, central pressure, and maximum sustained surface wind speed for all named Atlantic TCs from 1851 to the present (Jarvinen et al. 1984; Landsea et al. 2003). The SHIPS database contains synoptic information every 12 h for all Atlantic basin tropical cyclones that developed from 1989 to the present. Most of the Table 1 variables are used as predictors in the SHIPS model; however, a few variables that are not explicitly employed in SHIPS are also included in the table. Each variable was evaluated at the beginning (t = 0 h) of each 24-h period in the database provided that the system remained both over water and tropical (e.g., extratropical and subtropical cases were excluded) during the period from t − 12 h

to $t + 24$ h. The determination as to whether or not these criteria were satisfied was made using the NHC HURDAT file. Since nondeveloping depressions are not included in the current version of that file, a modified version of the HURDAT file that contained these systems was created. The nondeveloping depression information required to construct the updated HURDAT file was obtained from the NHC B decks (J. M. Gross 2001, personal communication). For the purpose of this study, a system that remained over land for ≤1 h was designated as an over-water system so that TCs that grazed the coastline were not excluded from the database.

The HURDAT file was utilized to evaluate the climatological and persistence variables listed in Table 1. The magnitudes of the maximum sustained surface wind (VMX), latitude (LAT), and longitude (LON) were extracted directly from the HURDAT file. The variable JDAY was evaluated by taking the absolute value of the difference between the Julian date at time $t = 0$ h and the Julian date of the peak day of the hurricane season (Julian date 253 = 10 September) as determined previously by Neumann et al. (1999). The magnitude of the previous 12-h change in maximum wind speed (DVMX) was evaluated by subtracting VMX at $t = 0$ h from VMX at $t = -12$ h. The u component of the storm motion (USTM) and the storm speed (SPD) were evaluated for the 12-h period centered on the initial ($t = 0$ h) time of each 24-h period. The 24-h change in VMX (ΔV_{24}) was also determined for each 24-h time period by subtracting VMX at $t + 24$ h from VMX at $t = 0$ h. This was not included in Table 1, since it is the variable we are trying to predict while the variables in Table 1 are predictors.

The methodology currently used to compute the synoptic oceanic variables is identical to that described in DK99. Briefly, the observed sea surface temperature (SST) at each initial TC location was determined from the most recent Reynolds and Smith (1993) gridded 1.0° latitude–longitude weekly analysis available prior to storm passage. The empirically derived maximum potential intensity (MPI) was determined by

$$\text{MPI} = \min[X, 85], \tag{1}$$

where

$$X = A + B(\exp)[C(\text{SST} - \text{SST}_0)] \quad \text{and}$$

$$A = 34.2 \text{ m s}^{-1}, \qquad B = 55.8 \text{ m s}^{-1},$$

$$C = 0.1813^\circ\text{C}^{-1}, \quad \text{and} \quad \text{SST}_0 = 30^\circ\text{C}.$$

The constant A includes a mean translational speed of 6 m s^{-1} for Atlantic TCs. For a more complete description of the derivation of the MPI, consult DeMaria and Kaplan (1994b). The storm potential variable (POT) was determined by subtracting VMX at $t = 0$ h from the MPI determined from (1).

The procedures that are currently employed to evaluate many of the SHIPS atmospheric variables listed in Table 1 differ somewhat from those described in DK99. The SHIPS atmospheric predictors are still evaluated using the 0000 and 1200 UTC Aviation Model (AVN) fields (Caplan et al. 1997) sampled at 2.0° (2.5° prior to 1996) latitude–longitude at the mandatory levels from 1000 to 100 hPa (except 925 hPa) as discussed in DK99. However, the storm vortex is no longer removed from the $t = 0$ h analysis as was done previously (see DK99). As a result, the averaging domain used for several of the atmospheric variables was changed so that evaluation of the environmental variables is not contaminated by the storm vortex. In the current version of SHIPS, the vertical shear (SHR) is now determined by subtracting the 850- and 200-hPa wind vectors averaged from radius (r) = 200–800 km. Previously, the SHR was computed from $r = 0$–600 km. The magnitudes of the u component of the 200-hPa wind (U200) and the 200-hPa temperature (T200) are obtained by averaging each of these variables from $r = 200$–800 km. Previously, they were averaged from $r = 0$–1000 km. The methodology used to compute the 850-hPa relative vorticity (Z850) and the relative eddy flux convergence (REFC) is the same as described in DK99. Briefly, Z850 is obtained by averaging the magnitude of Z850 from $r = 0$–1000 km while the REFC is evaluated using

$$\text{REFC} = -r^{-2}\frac{\partial}{\partial \text{r}}(r^2\overline{U_L'V_L'}), \tag{2}$$

where r is the radius from the center, and U and V are the 200-hPa radial and tangential winds, respectively. The overbar denotes an azimuthal average, the prime denotes a deviation from the azimuthal mean, and the subscript L indicates that the storm motion has been subtracted from the winds. The REFC is evaluated at 100-km intervals using (2) and then averaged from $r = 100$–600 km to obtain the REFC variable used in SHIPS. A few predictors that were not included in DK99 have been added recently to the SHIPS model. The first of these new predictors is the 850–700-hPa relative humidity (RHLO) averaged from $r = 200$–800 km. In addition, the steering layer (SLYR) that represents the center of mass of the layer where the environmental winds best match the current storm motion vector averaged from $r = 200$–800 km is also included as a SHIPS predictor.

Since the SHIPS database (DK99) only contains synoptic information every 12 h, the 0000 and 1200 UTC predictor values were averaged to estimate the magnitude of the corresponding SHIPS variables at 0600 and 1800 UTC. Each of the Table 1 variables was evaluated for 163 TCs [30 tropical depressions (VMX < 18 m s^{-1}), 54 tropical storms (18 m s^{-1} ≤ VMX ≤ 32 m s^{-1}), and 79 hurricanes (VMX ≥ 33 m s^{-1})]. These TCs contributed a total of 2621 cases (e.g., 24-h time periods) that were subsequently employed in the statistical analyses discussed in sections 3 and 4.

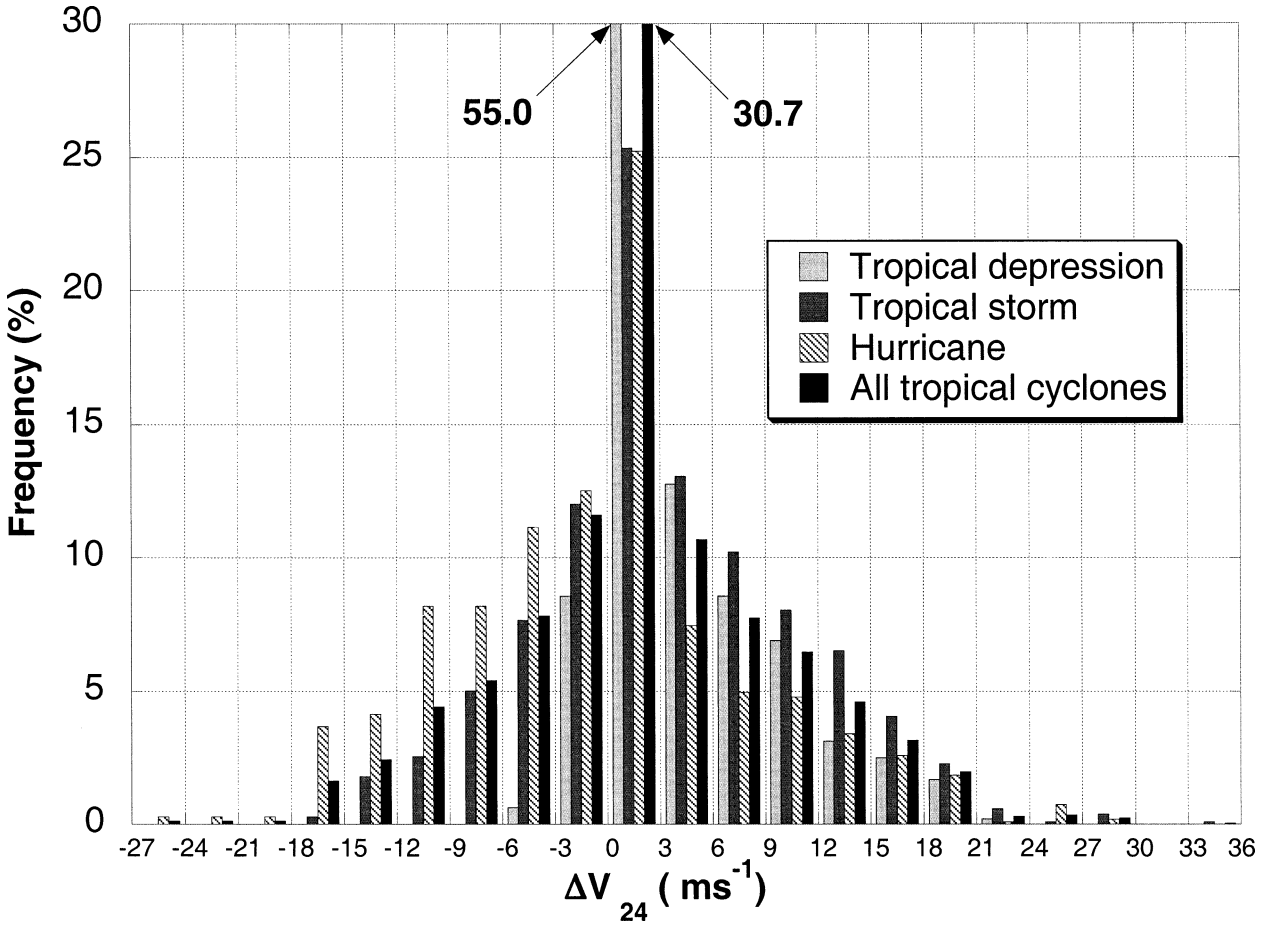

FIG. 1. The frequency distributions of 24-h intensity change (ΔV_{24}) stratified by tropical cyclone intensity at time $t = 0$ h. The distributions are provided for tropical depressions (VMX < 18 m s^{-1}), tropical storms (18 m s$^{-1} \leq$ VMX ≤ 32 m s^{-1}), hurricanes (VMX ≥ 33 m s^{-1}), and all tropical cyclones.

3. Intensity change distribution

Figure 1 shows the frequency distributions of ΔV_{24} as a function of the initial ($t = 0$ h) intensity of all 2621 cases. Slow intensification ($0 \leq \Delta V_{24} < 3$ m s^{-1}) was the most frequently observed 24-h intensity change for each of the intensity classes. The figure indicates that a higher fraction of the tropical storm sample than of the hurricane or tropical depression sample exhibited ΔV_{24} changes exceeding 3 m s^{-1}. This finding may be attributable to a few different factors. First, tropical storms are further from their MPI than hurricanes and, thus, have the potential to intensify faster. Also, tropical storms may intensify more than tropical depressions because of their better initial organization. In contrast, Fig. 1 indicates that hurricanes are more likely to decay at a fast rate than either tropical storms or tropical depressions. This is consistent with the higher initial intensities and hence the increased potential of hurricanes to decay quickly. Figure 2 shows the cumulative frequency distributions of ΔV_{24} for each of the intensity classes. Although TC decay ($\Delta V_{24} < 0$) occurs for ~50% of all hurricane cases, it only occurred in ~10% of the tropical depression cases, ~30% of the tropical storm cases, and ~35% of all tropical cyclone cases. Table 2 summarizes the ΔV_{24} distributions shown in Fig. 1. The table shows that the mean change in ΔV_{24} was positive for tropical storms and depressions, and slightly negative for hurricanes. Table 2 also shows that the hurricane cases had a larger intensity range and standard deviation than either the tropical storm or tropical depression sample. In addition, the hurricane sample exhibited the largest decreases in ΔV_{24} of any of the intensity classes. The latter finding may be due, in part, to the comparatively high initial intensities of the hurricane cases as suggested previously. Alternatively, this may reflect a higher likelihood for hurricanes to weaken significantly due to the collapse of an inner eyewall, since Willoughby et al. (1982) showed that concentric eyewalls occurred more frequently in intense TCs.

The goal of this study is to determine if the large-scale conditions associated with the RI cases were significantly different from those that were present for cases that did not experience RI (non-RI cases). In this study, RI is defined as the 95th percentile of ΔV_{24} for

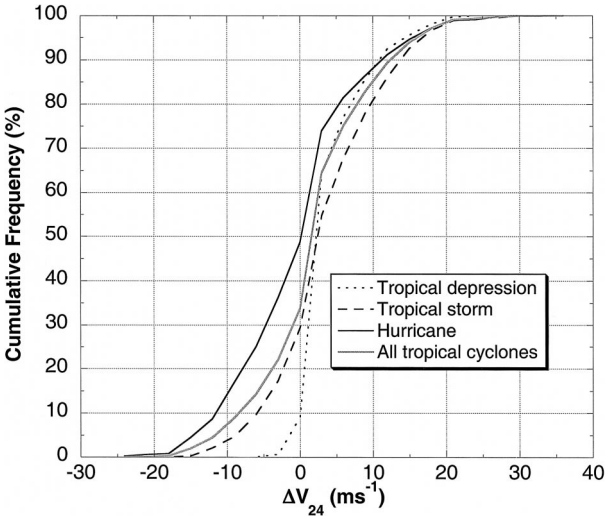

FIG. 2. Same as in Fig. 1 except for the cumulative frequency distributions.

all of the TC cases used in this study (see Fig. 2). Although the 95th percentile of the ΔV_{24} distribution is 16.0 m s^{-1}, an RI threshold of 15.4 m s^{-1} (30 kt) is employed in this study since it is in better agreement with the 16.0 m s^{-1} threshold than the next-closest ΔV_{24} change of 18.0 m s^{-1} (35 kt) due to the 2.6 m s^{-1} (5 kt) resolution of the HURDAT file. Figure 2 shows that the 95th percentile of ΔV_{24} was similar for the different intensity classes. Thus, employing one RI threshold regardless of initial intensity is viewed as a reasonable assumption. It is interesting to note that the Holliday and Thompson (1979) definition for RI of a 24-h pressure fall of $\geq$42 mb is equivalent to the 99.7th percentile of all of the 24-h pressure changes of the TCs (tropical depressions, tropical storms, and hurricanes) in the current study sample.

The RI sample employed in this study was comprised of 50 TCs compared with the sample total of 163 TCs. These 50 TCs contributed a total of 159 RI cases, since it was possible for a TC to undergo RI more than once during its lifetime. Table 3 shows the distribution of the RI cases as a function of the initial TC intensity. The table shows that systems that were initially of tropical storm intensity accounted for the largest percentage of RI cases while hurricanes contributed the next largest

TABLE 2. The 24-h intensity change (ΔV_{24}) statistics of the tropical depression, tropical storm, hurricane, and all tropical cyclone intensity classes. The number of cases (N), mean, standard deviation (std dev), minimum (min), and maximum (max) ΔV_{24} are also provided.

Intensity class	N	Mean (m s^{-1})	Std dev (m s^{-1})	Min (m s^{-1})	Max (m s^{-1})
Hurricane	1086	−0.7	8.6	−25.7	28.3
Tropical storm	1057	3.2	7.6	−15.4	33.4
Tropical depression	478	3.4	4.9	−5.1	23.1
All tropical cyclones	2621	1.6	7.9	−25.7	33.4

TABLE 3. The distribution of 24-h intensity change (ΔV_{24}) for the 159 RI cases stratified by intensity class. The number of RI cases for each range of ΔV_{24} are also provided. The total number of RI cases and the percentage of the RI sample total contributed by each of the intensity classes are also presented.

ΔV_{24} (m s^{-1})	Tropical depressions	Tropical storms	Hurricanes	All tropical cyclones
15.4–18	12	43	28	83
18–21	8	24	20	52
21–24	1	6	1	8
24–27	0	1	8	9
27–30	0	4	2	6
30–33	0	0	0	0
33–36	0	1	0	1
Total cases (%)	21 (13.2)	79 (49.7)	59 (37.1)	159 (100.0)

percentage and tropical depressions the smallest percentage. Although this result is partly due to variations in the sizes of each of the intensity classes, the likelihood for RI is still greatest for tropical storms and lowest for tropical depressions when the number of RI cases (see Table 3) in each intensity class is normalized by class sample size (see Table 2). Specifically, 4.4%, 7.4%, and 5.4% of the tropical depression, tropical storm, and hurricane samples underwent RI, respectively. Table 3 also indicates that the tropical storm cases composed the largest number of cases in which ΔV_{24} exceeded 27 m s^{-1}. The sample total of 159 RI cases represents ~6% of the sample of 2621 cases. The mean ΔV_{24} of these RI cases is 18.2 m s^{-1}, which corresponds to about two categories on the Saffir–Simpson hurricane scale (Saffir 1973; Simpson 1974). Although the number of 24-h time periods when RI occurred was rather low, the percentage of systems that underwent RI at least once during their lifetime was considerably larger. Figure 3 indicates that nearly 60% of all systems that attained hurricane strength, 83% of all systems that reached major hurricane intensity (VMX $\geq$ 50 m s^{-1}), and all category

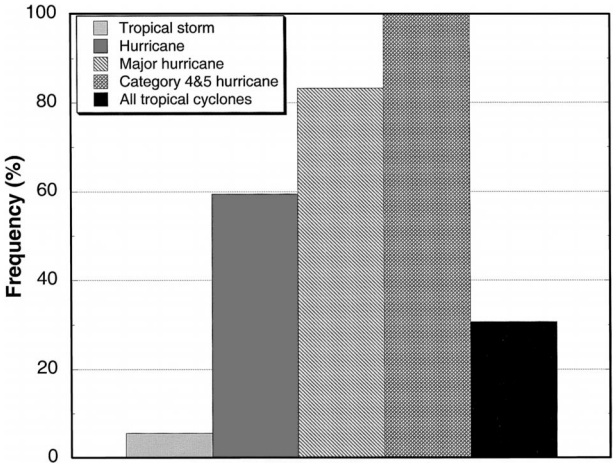

FIG. 3. The percentage of systems that underwent RI at least once during their lifetime as a function of the maximum intensity attained by each system.

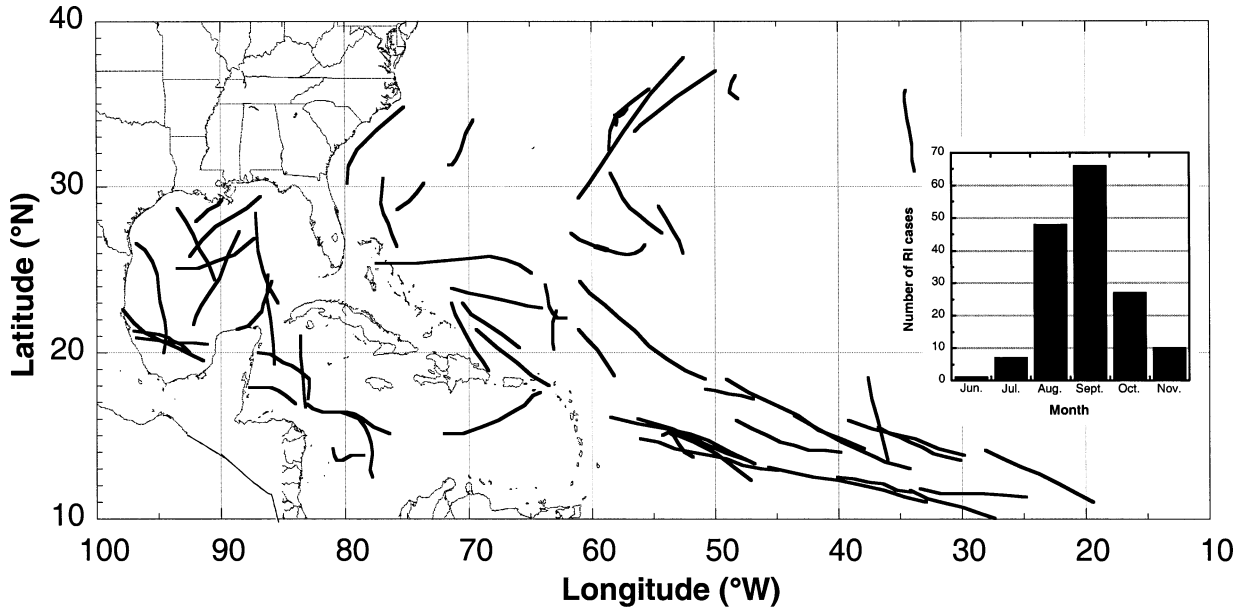

FIG. 4. The 24-h tracks of the 1989–2000 RI cases. The distribution of the RI cases by the month when they occurred is also presented.

4 (VMX $\geq$ 59 m s^{-1}) and category 5 (VMX $\geq$ 70 m s^{-1}) hurricanes underwent RI at least once during their lifetime. Overall, 31% of all Atlantic TCs and 38% of all named storms underwent RI.

Figure 4 shows the 24-h tracks of the RI cases. Since RI may occur for consecutive 24-h time periods, some of the tracks overlap. The figure indicates that RI generally occurred south of 30°N. Also, there appears to be a tendency for fewer RI cases in the eastern Caribbean and the eastern Gulf of Mexico. Analysis of the tracks of all 2621 cases (not shown) suggests that the lack of RI tracks in the eastern portion of the Caribbean may result, in part, from a lower frequency of TCs in that region. However, this does not appear to be a plausible explanation for the lack of RI cases in the eastern Gulf of Mexico, since the TC tracks appear rather evenly distributed within that basin. Clearly, the large-scale environment plays a role in determining which regions are favored for RI. In the succeeding section, the large-scale conditions that are conductive to RI will be examined in more detail.

Figure 4 also shows the seasonal distribution of the RI cases. The vast majority of the RI cases (72%) occurred in August and September. Interestingly, a much larger fraction of the RI cases occurred in October and November (23%) than in June and July (5%). This is consistent with the analysis of Neumann et al. (1999) who showed that tropical cyclones occur more frequently in the months of October and November than June and July.

TABLE 4. As in Table 1 except for the mean magnitudes of the initial (t = 0 h) climatological and synoptic variables of the RI and non-RI samples. The differences between these mean values (D = RI − non-RI) are also shown. A single, double, or triple asterisk was placed in parentheses beside a D value if the results of a two-sided t test indicated that this difference was statistically significant at either the 95% (*), 99% (**), or 99.9% (***) level. The RI (N = 159) and non-RI (N = 2462) sample sizes that were used to perform all significance tests were adjusted for serial correlation between cases (see N_e values below).

Variable	Units	RI (N = 159, N_e = 92)	Non-RI (N = 2462, N_e = 705)	D = RI − non-RI
VMX	m s^{-1}	28.9	30.1	−1.2
LAT	°N	19.7	23.4	−3.7 (***)
LON	°W	63.2	57.2	6.0 (*)
SPD	m s^{-1}	5.2	5.3	−0.1
DVMX	m s^{-1}	4.6	1.0	3.6 (***)
USTM	m s^{-1}	−3.1	−1.8	−1.3 (**)
JDAY		22.5	25.0	−2.5
SST	°C	28.4	27.5	0.9 (***)
POT	m s^{-1}	47.6	40.3	7.3 (***)
SHR	m s^{-1}	4.9	8.5	−3.6 (***)
U200	m s^{-1}	−0.6	3.8	−4.4 (***)
T200	°C	−53.3	−53.4	0.1
RHLO	%	69.7	65.4	4.3 (***)
Z850	10^{-7} s^{-1}	32	22	10.0
REFC	m s^{-1} day^{-1}	0.9	2.4	−1.5 (**)
SLYR	hPa	583.4	613.2	−29.8 (**)

4. Large-scale conditions associated with RI and non-RI cases

a. Comparison of initial conditions

In this section, the large-scale conditions present at the start of each of the 159 episodes of RI are compared to those present at the beginning of the 2462 non-RI cases to determine if the initial conditions for these two samples were significantly different (the distribution of these conditions is discussed in section 4b). Table 4

shows the mean initial values of each of the variables listed in Table 1 for both the RI and non-RI samples. The differences between the mean magnitudes of the RI and non-RI samples are also presented in the table. Asterisks were placed beside those differences that were determined to be statistically significant at the 95% (*), 99% (**), or 99.9% (***) level using a two-sided *t* test that assumes unequal variances (Dowdy and Wearden 1991). Prior to computing the *t* statistic and the corresponding degrees of freedom, the RI and non-RI sample sizes were adjusted for serial correlation between cases to obtain the effective sample size (N_e) following the methodology described in Aberson and DeMaria (1994). This was necessary since many of the cases used in this study occurred during consecutive time periods and successive tropical cyclone observations are correlated and should not be considered independent. In Aberson and DeMaria (1994), all of the computations required to determine N_e were made using track forecast errors as the dependent variable. However, the present study employs 24-h intensity change as the dependent variable as suggested by C. J. Neumann (2000, personal communication).

Table 4 indicates that statistically significant differences exist between the RI and non-RI samples for several of the climatological and persistence variables. However, these differences are not, on average, as significant as the differences that were computed for the synoptic variables. Specifically, the systems that underwent RI tended to be located farther south and west than the systems that did not undergo RI. Also, the RI cases tended to have a more westerly component of motion than the non-RI cases. The above findings are consistent with the climatologically higher SSTs in the south and western portions of the Atlantic basin (Levitus 1982), since Table 4 also indicates that high SST was characteristic of the RI cases. Finally, the RI cases were generally intensifying at a faster rate than the non-RI cases during the 12-h period prior to the onset of RI.

Table 4 also indicates that statistically significant differences were not found between the VMX, JDAY, and SPD values of the RI and non-RI samples. It is not surprising that JDAY and VMX are not good indicators of RI since the RI cases occur during most of the hurricane season (Fig. 4) and over a wide range of initial intensities (as will be shown in section 4b). The similarity in the initial SPD of the RI and non-RI cases is somewhat surprising in light of the study by Schade and Emanuel (1999) that showed a strong relationship between storm speed and the magnitude of the negative feedback between the ocean and the TC vortex. However, Cione and Uhlhorn (2003) show that systems that displayed the highest degree of inner-core cooling were moving at nearly the same speed as the remainder of the sample. Consequently, other factors (e.g., mixed layer depth) may play a more important role than SPD in determining the magnitude of the negative feedback between the ocean and the TC vortex.

Statistically significant differences were found between the magnitudes of the RI and non-RI cases for all of the synoptic variables, except for T200 and Z850. The most statistically significant differences (i.e., the 99.9% level) were found for SST, RHLO, POT, SHR, and U200. Table 4 shows that the RI cases had higher values of SST, RHLO, and POT. The finding that RI occurred in regions with warmer SSTs seems consistent with the Carnot theory described in Emanuel (1988) and the empirical results of DeMaria and Kaplan (1994b). Both studies found that higher storm intensities are possible for warmer SSTs and these higher intensities would presumably increase the possibility for a TC to experience large rates of intensification. Although the finding of larger RHLO values for the RI cases seems consistent with physical reasoning, they are at odds with Schade and Emanuel (1999) who found that lower boundary layer relative humidity in the initial undisturbed environment actually produced the most intense storms in their model simulations. They speculated that this finding was due to a stronger disequilibrium at the sea surface for drier boundary layers. However, since RHLO was evaluated from 700 to 850 hPa in the current study, our results are not entirely comparable to those of Schade and Emanuel (1999) whose model simulations utilized boundary layer relative humidity. The finding of higher POT values for the RI cases seems reasonable since from a purely algebraic viewpoint systems with initial intensities that were further from their MPI would have a greater opportunity to intensify rapidly.

The finding of lower values of SHR for the RI cases is consistent with the results of DeMaria and Kaplan (1994a). It is also consistent with the three-dimensional modeling simulations of Frank and Ritchie (1999) that showed that a TC embedded in an environment with no shear intensified rapidly. Table 4 shows that the RI cases were situated in a more easterly 200-hPa flow. Since a fairly high linear correlation was found between U200 and SHR ($r = 0.71$), this result may be due, in part, to the increased likelihood for storms that are embedded in upper-level easterly flow to be in a low shear environment. Alternatively, the recent results of Frank and Ritchie (2002) suggest that for TCs in the Northern Hemisphere upper-level easterly flow may counteract the low-level southeast flow that is produced by the so-called beta gyres thereby reducing the net shear over the storm.

Statistically significant differences at the 99% level were found between the initial REFC and SLYR values of the RI and non-RI cases. Specifically, the RI cases had lower values of REFC and SLYR than the non-RI cases. The finding of low REFC for the RI cases is consistent with the study by Hanley et al. (2001) who showed that systems were more likely to experience high rates of intensification if they did not interact with a trough. The lower values of SLYR indicate that systems that are moving with the environmental wind within a higher layer in the atmosphere are more likely to

undergo RI. One plausible explanation for this result is that systems that follow the flow within a higher layer of the atmosphere are less likely to be adversely affected by the strong low-level (~700–850 hPa) easterly surges associated with the Saharan air layer. Dunion and Velden (2002) hypothesize that these low-level surges are often accompanied by very dry air and high vertical wind shear, both of which are detrimental to TC intensity.

Since the conditions that are most favorable for RI may vary somewhat as a function of TC intensity, the mean initial conditions of the RI and non-RI samples were computed for the three intensity classes (e.g., tropical depression, tropical storm, and hurricane). The differences between the mean initial conditions of these three classes were computed and the statistical significance of these differences were evaluated following the procedures described previously in this section. This analysis (not shown) indicates that the initial conditions associated with the hurricane and tropical storm RI samples were fairly similar. However, due to the stratification process itself, the hurricane RI sample had larger values of VMX and lower values of POT than the tropical storm RI sample. In addition, the DVMX values of the hurricane RI sample were larger than those of the tropical storm RI sample. The differences between the VMX, POT, and DVMX values of the hurricane and tropical storm RI samples were significant at the 95% level.

A comparison of the mean initial conditions of the tropical depression RI sample to those of the tropical storm and hurricane RI samples indicates that the tropical depression RI cases had a smaller westward component of motion and higher values of SHR, U200, and REFC. These differences were all significant at the 95% level or greater, except for the differences between the REFC values, which were significant at the 90% level. This suggests that the conditions that are favorable for tropical depressions to undergo RI may be somewhat different from those that are favorable for hurricanes and tropical storms. Specifically, the higher values of SHR, U200, and REFC may indicate that trough interactions play a more important role in the RI process of tropical depressions than they do for tropical storms and hurricanes. Nevertheless, although the mean REFC of the tropical depression RI cases was greater than the total study sample (2621 case) average REFC, the mean SHR and U200 of the tropical depression RI cases were still less than the corresponding sample average values of SHR and U200. This suggests that relatively favorable environmental flow patterns (e.g., vertical shear) are also necessary for upper-level troughs to have a positive impact on TC intensity as suggested by DeMaria et al. (1993). Nevertheless, since the sample sizes of the three different RI classes were fairly small, more cases will be required to confirm the above hypothesis.

b. Distribution of large-scale conditions

The results in section 4a show that statistically significant differences exist between the mean initial conditions of the RI and non-RI samples for many of the variables listed in Table 1. In this section, the distributions of these initial conditions are shown for all of the Table 1 variables for which statistically significant differences were found between the RI and non-RI samples as well as for a few other variables of interest. The frequency distributions are shown for both the RI and non-RI samples so that comparisons can be made between the relative likelihood that RI will occur for any given range of predictor magnitudes.

Figure 5 shows the frequency distributions of the RI and non-RI cases for several of the climatological and persistence variables in Table 1. The figure shows that the frequency distributions of VMX are quite similar for the RI and non-RI samples, which is consistent with the lack of statistically significant differences between the sample mean RI and non-RI VMX values (Table 4). However, the figure does indicate that the distribution of RI cases is more skewed toward low VMX values than the distribution of non-RI cases. This seems reasonable since when VMX is high, systems are closer to their MPI and thus have less of an opportunity to intensify significantly. The distributions of DVMX are quite different for the RI and non-RI samples with a much larger fraction (97% versus 77%) of the RI than non-RI cases intensifying during the previous 12 h. Also, the fraction of RI cases that were intensifying at high rates ($\Delta V_{24} \geq 3$ m s^{-1}) was substantially larger than was observed for the non-RI cases.

Figure 5 shows notable differences between the distributions of LAT and LON for the RI and non-RI samples. Rapid intensification occurs most frequently from 10° to 15°N, and the fraction of RI cases generally decreases with increasing LAT. In contrast, the non-RI cases occur most frequently from 15° to 20°N and exhibit a much slower poleward decrease. The distributions of LON values for the RI and non-RI cases indicate a preference for RI to commence east of 40°W and from 80° to 100°W, in the far eastern Atlantic and the western portions of the Caribbean and Gulf of Mexico basins, respectively. The preference for RI to occur in the far eastern Atlantic may simply be a reflection of systems getting organized and intensifying prior to reaching the mid-Atlantic trough. As discussed in Fitzpatrick et al. (1995), the mid-Atlantic trough (or TUTT) is a semipermanent feature in the North Atlantic basin during the months of June–October that can produce strong vertical wind shear that is detrimental to TC intensity. The relatively large concentration of RI cases in the northwestern Caribbean and the western Gulf of Mexico may be due, in part, to the deeper mixed layers in those regions (Lamb 1984).

Figure 5 shows that a larger fraction of RI cases than non-RI cases were moving westward (USTM < 0). The

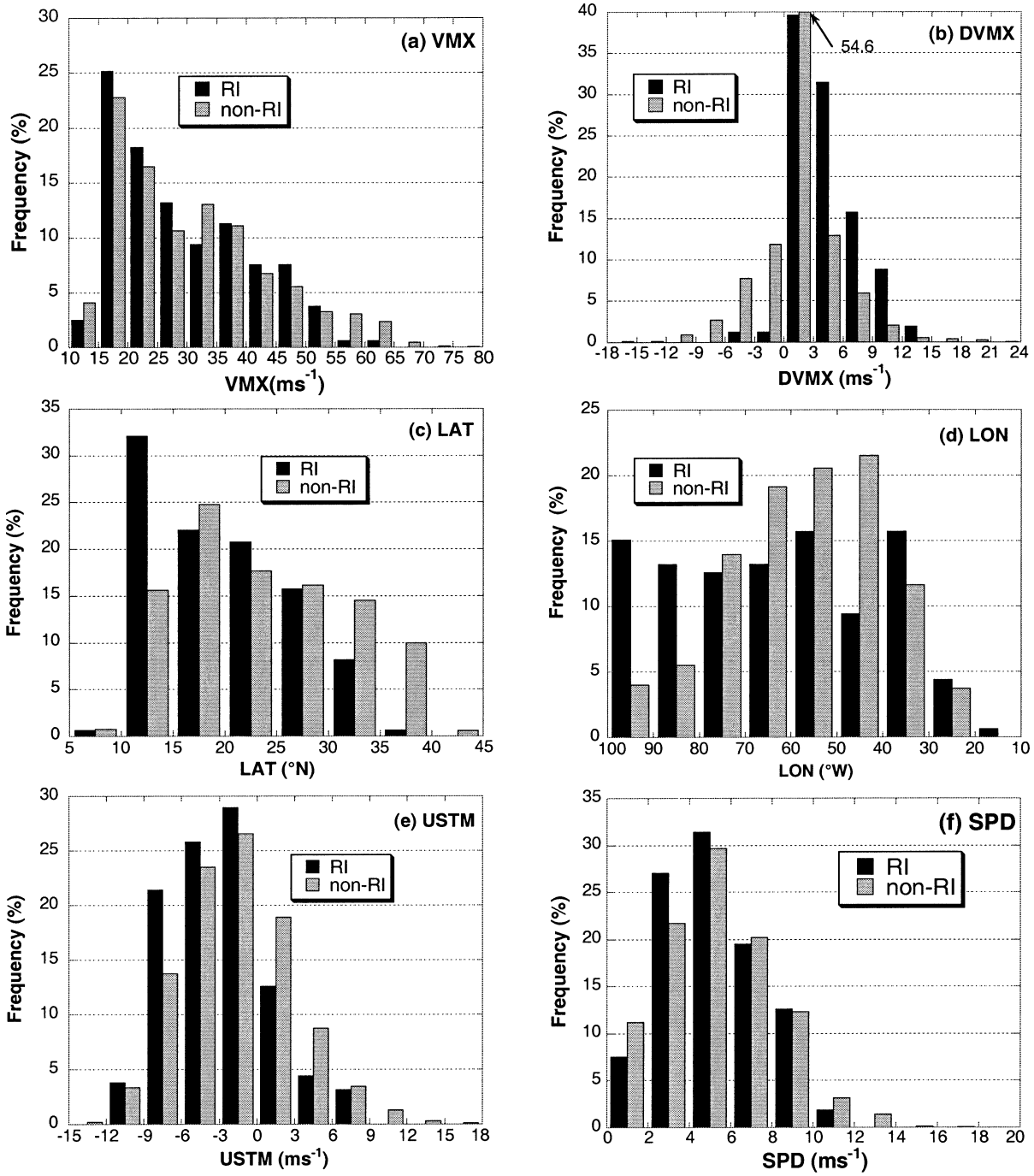

FIG. 5. Frequency distributions of the climatological and persistence variables for the RI and non-RI samples.

figure also indicates that the distribution of storms speeds for the RI and non-RI cases are quite similar. This is consistent with Holliday and Thompson (1979) who did not find a strong relationship between storm speed and the rapid development of northwest Pacific typhoons. Although RI was less likely for very slow storm speeds (SPD < 2 m s^{-1}), the majority (54%) of the RI cases occurred for storms moving slower than the total sample average SPD of 5.3 m s^{-1}. This suggests that while slow storm speeds may have a negative impact on TC intensity, other factors (e.g., deep mixed layers) can minimize this effect as suggested by Schade and Emanuel (1999).

Figure 6 shows the distribution of RI and non-RI cases for the thermodynamic variables. Substantial differences in the SST distributions of the RI and non-RI

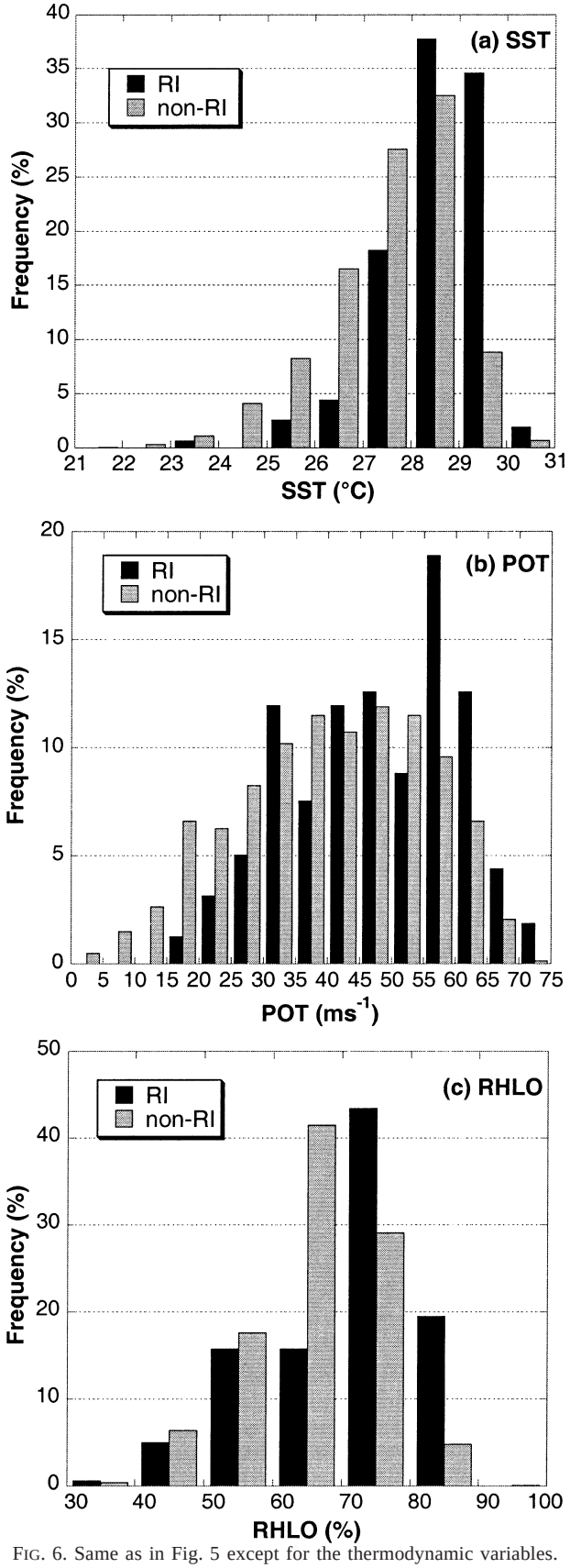

FIG. 6. Same as in Fig. 5 except for the thermodynamic variables.

samples are shown. These are most evident for SSTs above 29°C where the frequency of RI cases was nearly 4 times that observed for the non-RI sample. Nearly all (~92%) of the RI cases occurred for SSTs above 27°C. Analysis of the T200 values of the 12 RI cases with SSTs below 27°C indicates that all but one of these cases had T200 values colder than the mean of the total study sample (2621 cases). Furthermore, the mean T200 value of these 12 cases was more than two standard deviations colder than that of the total sample. Emanuel (1988) has shown that MPI is a function of SST, outflow temperature, and ambient relative humidity. Consequently, these findings suggest that very cold upper-level temperatures may have increased the MPI above what it ordinarily would have been for a particular SST. This enabled those systems to intensify at a more rapid rate than would otherwise have been possible. Rapid intensification is more likely to occur for large values of POT (Fig. 6). This finding is consistent with the aforementioned results that showed that RI was more likely to occur at high SSTs, since for any given VMX < 85 m s^{-1} a higher SST will yield a larger POT. A notable increase in the fraction of RI cases to non-RI cases was observed for large RHLO values (Fig. 6) with nearly two-thirds of all RI cases having RHLO exceeding 70% compared with only about one-third of non-RI cases. Also, approximately 4 times as many RI cases than non-RI cases had relative humidity values above 80%.

Figure 7 shows the frequency distribution of the RI and non-RI cases for the kinematic variables listed in Table 1. A substantial difference between the distributions of SHR of the RI and non-RI cases is seen. Specifically, 86% of the RI cases occurred when the SHR was less than 8 m s^{-1} (the total study sample mean SHR was 8.3 m s^{-1}) compared to 49% of the non-RI cases. Furthermore, 43% of the RI cases compared with 15% of the non-RI cases had SHR below 4 m s^{-1}. This suggests that low SHR is an important ingredient for RI. However, RI was also observed for moderate SHR values suggesting that other factors may compensate for increased SHR. Since the averaging area employed to compute SHR was fairly large, a region of high SHR may have existed outside the inner-core region in the moderate SHR cases. This region of high SHR may have increased the area-averaged SHR while having little detrimental impact on TC intensity. Also, Persing et al. (2002) have noted that SHR computed using the environmental wind at only two levels is unlikely to provide a complete assessment of SHR for any given storm. Finally, it is possible that external forcing from upper-level troughs or cold lows may have counteracted the detrimental effects of increased SHR for the RI cases with higher than average SHR. The mean REFC of the RI cases with above average SHR was 3.4 m s^{-1} day^{-1}, while the mean REFC of the total sample was only 2.3 m s^{-1} day^{-1}.

Substantial differences can be seen between the U200 distributions of the RI and non-RI samples (Fig. 7).

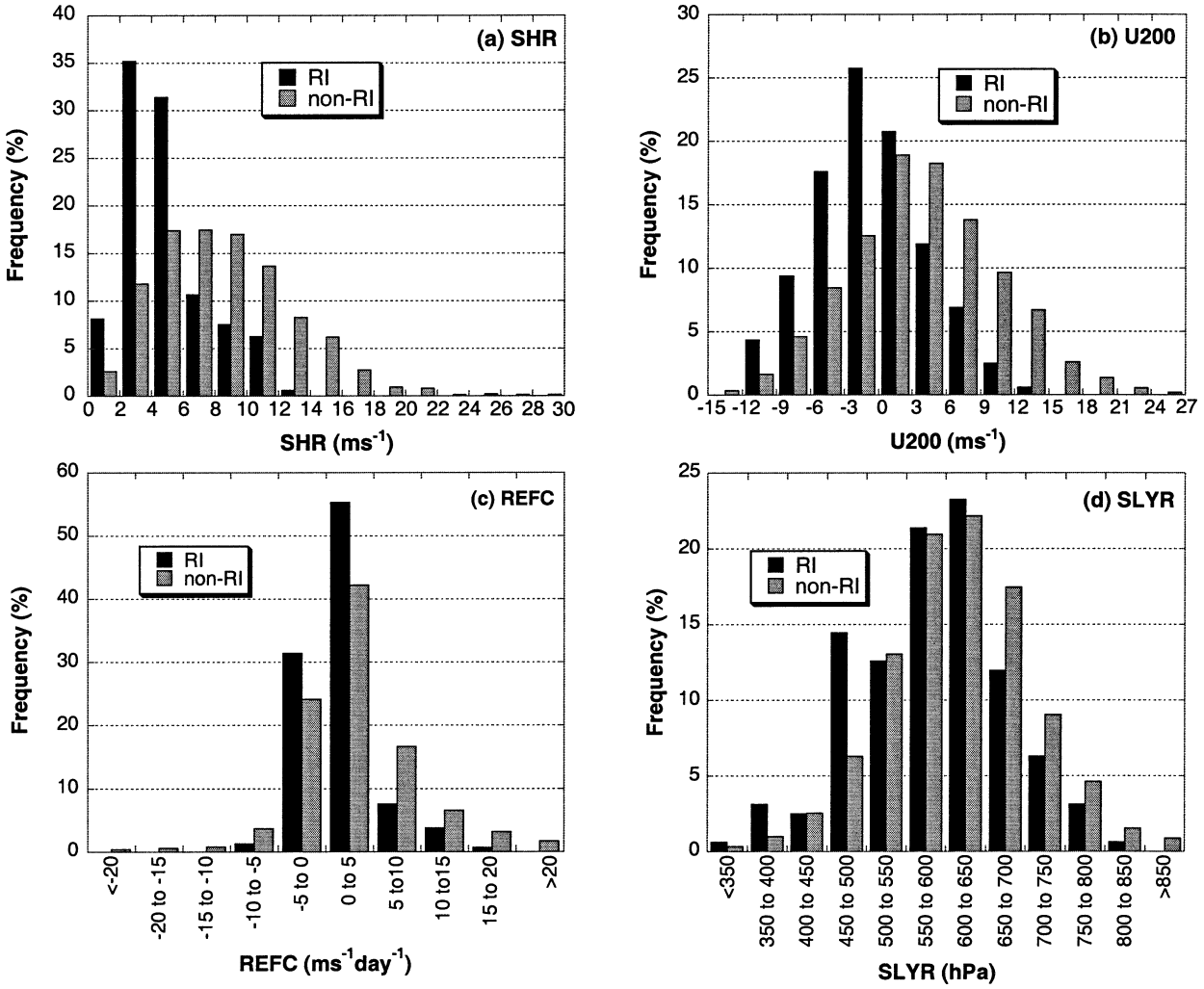

FIG. 7. Same as in Fig. 5 except for the kinematic variables.

Specifically, the distribution of U200 for the RI cases is skewed toward easterly environmental flow. Also, the largest fraction of RI cases occurred when U200 was weakly from the east. Since the low-level flow over much of the tropical northern Atlantic typically has an easterly component during the Atlantic hurricane season (Sadler et al. 1987), weak easterly flow at 200 hPa may be favored because it yields low SHR. Alternatively, Frank and Ritchie (2002) have suggested that upper-level easterly flow may counteract the low-level cross-vortex easterly flow induced by beta gyres, thereby minimizing the shear in the storm environment as noted earlier.

The majority of the RI cases were associated with weak REFC ($-5\ \mathrm{m\ s^{-1}\ day^{-1}} < \mathrm{REFC} < 5\ \mathrm{m\ s^{-1}\ day^{-1}}$) (Fig. 7). Also, large positive values of REFC were more likely to be associated with non-RI cases than with RI cases. This agrees with Hanley et al. (2001) who showed that large rates of intensification are less likely to occur when a system is interacting with an upper-level trough or cold low than when situated in a relatively quiescent environment as discussed previously. The RI cases also had lower values of SLYR (Fig. 7) and, thus tended to move with the flow at higher levels of the atmosphere than the non-RI cases. As noted previously, it is possible that systems that follow the low-level flow are less likely to undergo RI because they are more likely to be embedded in the Saharan air layer, which Dunion and Velden (2002) have suggested can have a detrimental impact on TC intensity.

c. Estimating the probability of RI

In this section, estimates of the probability of RI are obtained for each of the 11 Table 4 variables for which statistically significant differences were found at the 95% level or greater (section 4a) between the RI and non-RI samples. Probabilities were then computed by comparing each of the variables of the 2621 cases that composed the study sample to the corresponding RI

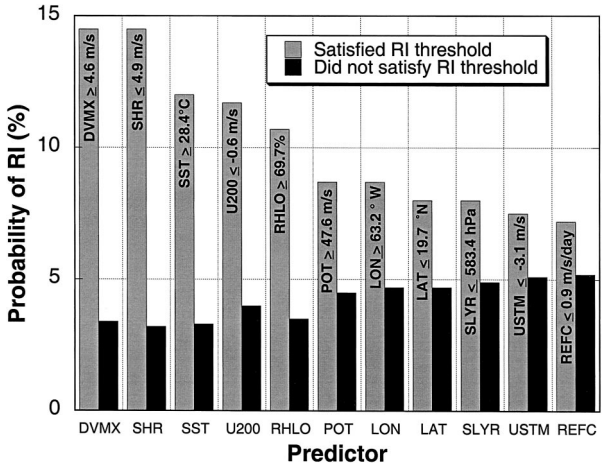

FIG. 8. The probability of RI when the specified RI predictors were satisfied for the RI and non-RI samples. The RI thresholds of each of the predictors are also presented.

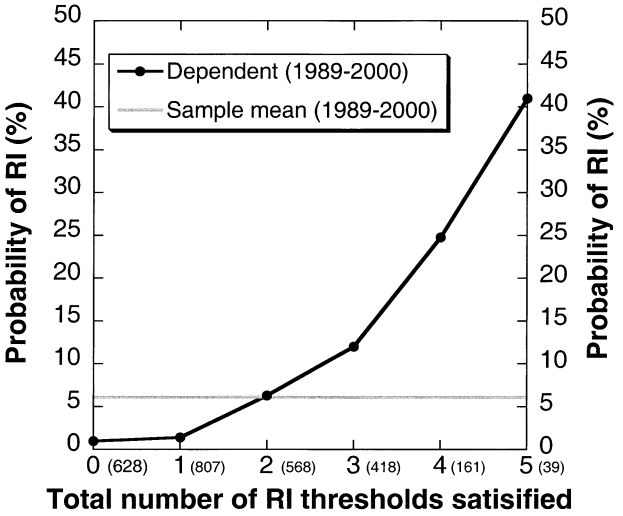

FIG. 9. The composite probability of RI determined for the 1989–2000-dependent sample. The probabilities are provided as a function of the total number of the five (DVMX, SHR, SST, POT, and RHLO) RI predictor thresholds that were satisfied. The sample mean probability of RI is also shown for reference. The number of cases is shown in parentheses beside the total number of RI thresholds satisfied.

threshold. The RI threshold for each variable was defined as the RI sample mean (Table 4). A threshold was said to be satisfied if a value was either $\leq$ or $\geq$ the specified RI threshold, whichever the previous analysis (section 4a) had shown was favorable for RI. For example, the RI sample had a mean DVMX of 4.6 m s^{-1}. Thus, the DVMX RI threshold was satisfied when DVMX was $\geq$4.6 m s^{-1}.

Figure 8 shows the probability of RI for each of the variables for which statistically significant differences were found to exist between the means of the RI and non-RI samples. These RI probabilities were obtained by dividing the number of RI cases that satisfied a given RI threshold by the number of cases in the entire sample (2621 cases) that satisfied that same threshold. To illustrate, RI occurred 92 times when the threshold for DVMX was satisfied, but the DVMX threshold was satisfied a total of 633 times. Thus, the probability of RI was 15% (92/633) when the RI threshold for DVMX was satisfied. The figure shows that the probability of RI ranged from 7% when the threshold for REFC was satisfied to 15% when the thresholds for DVMX or SHR were met. For comparison, the sample mean probability of RI is 6% (159 RI cases/2621 total cases). It is worth noting that the probability of RI when an RI threshold was satisfied exceeded the probability of RI when an RI threshold was not satisfied for each of the 11 predictors (Fig. 8). Also, these RI probabilities were all larger than the sample mean probability of RI. This suggests that this simple technique does provide additional information over that which is provided by climatology.

Since the probability of RI for any individual predictor was not particularly high, various sets of predictors were combined in an attempt to provide improved probability of RI estimates. Predictors that were statistically significant at the 95%, 99%, and 99.9% levels were employed to obtain a composite estimate of the probability of RI. It was found that employing the set of predictors that were significant at the 99.9% level yielded the highest RI probabilities. However, the variation of the probability of RI as a function of the total number of thresholds satisfied was somewhat noisy. Sensitivity tests showed that excluding LAT and U200 yielded improved probability of RI estimates. This is likely due, in part, to the finding that these variables were rather highly correlated with other predictors that had higher individual RI probabilities. Specifically, it was determined that U200 was rather highly correlated with SHR, and LAT was correlated with SST and POT. Figure 9 shows the composite probability of RI for the 1989–2000-dependent dataset obtained using the remaining five predictors (DVMX, SHR, SST, POT, RHLO). The probability of RI increased from 1% to 41% when the total number of thresholds (out of five) satisfied increased from zero to five, and was close to the sample (climatological) mean value of 6% when two thresholds were satisfied. The figure also indicates that a total of five RI thresholds were satisfied for $<$2% of the total sample, which suggests that TCs are rarely situated in an environment where synoptic conditions conducive to RI are present simultaneously. Nevertheless, a disproportionately large percentage ($\sim$10%) of the sample total number of RI cases were observed when all five of the RI thresholds were satisfied, which underscores the importance of those five conditions to the RI process. Since the probability of RI was 41% when all five of the RI predictors were satisfied (Fig. 9) and the highest probability of RI for any single predictor was only 15% (Fig. 8), this emphasizes the need to

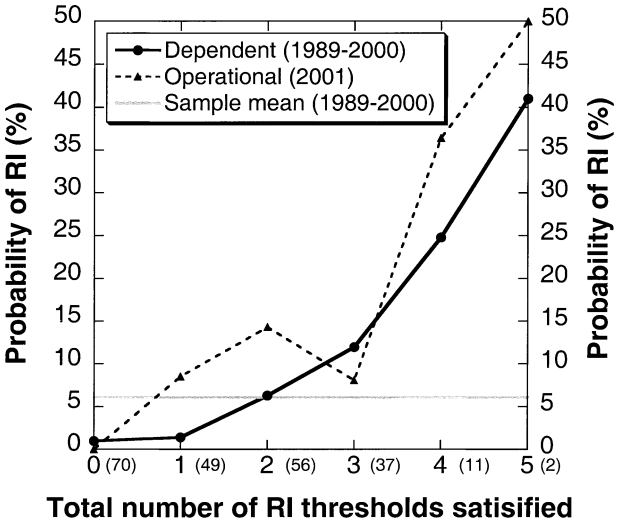

FIG. 10. Same as in Fig. 9 except that the operational probability of RI estimates obtained during the 2001 Atlantic hurricane season are also depicted. The number of cases for the 2001 season is provided in parentheses beside the total number of RI thresholds satisfied.

include (examine) the effects of a wide range of physical processes when predicting (studying) RI.

Figure 8 shows that the probability of RI ranged from 7% to 15% when one threshold was satisfied, while Fig. 9 indicates that the probability of RI was $<2\%$ when one of the five thresholds was satisfied. This apparent discrepancy arises because the RI probabilities shown in Fig. 9 were computed by determining the total number of thresholds that were satisfied out of the maximum possible total of five, while those shown in Fig. 8 were calculated separately for each of the 11 predictors.

Commencing on 2 August 2001, the simple technique described above was provided to NHC in real time during the 2001 Atlantic Hurricane season in support of the Joint Hurricane Testbed (JHT) that supports the transition of research results to operations. Figure 10 shows the probability of RI estimates obtained during the 2001 Atlantic hurricane season as well as those obtained for the 1989–2000-dependent sample. Although the 2001 sample size was fairly small, (especially when four or five thresholds were satisfied) the RI probabilities computed operationally during the 2001 Hurricane season were similar to those obtained for the 1989–2000-dependent sample. These results are encouraging and suggest that this simple technique has the potential to provide useful information to forecasters. Indeed, NHC forecasters sometimes utilized the aforementioned estimates of the probability of RI operationally during the 2001 hurricane season. Future work will focus on attempting to improve the probability of RI estimates by employing additional predictors such as upper-ocean heat content (Shay et al. 2000) and Geostationary Operational Environmental Satellite (GOES) infrared satellite imagery (Fitzpatrick 1997) that previous research suggests may be linked to RI. Also, more sophisticated statistical methods [e.g., neural network; Baik and Hwang (1998)] for estimating the RI probabilities will be explored.

5. Concluding remarks

The primary findings of this study are as follows.

- A definition for rapid intensification (RI) for Atlantic tropical cyclones was proposed. In this study, RI was defined as approximately the 95th percentile of all 24-h over-water intensity changes of Atlantic basin tropical cyclones that developed from 1989 to 2000. This equated to a maximum sustained surface wind speed increase of 15.4 m s^{-1} (30 kt) over a 24-h period.
- Of the 163 tropical cyclones that composed the 1989–2000 sample, 31% of all tropical cyclones, 60% of all hurricanes, 83% of all major hurricanes, and all category 4 and 5 hurricanes underwent RI at least once during their lifetime.
- The RI cases tended to occur farther south and west than the non-RI cases. In addition, the RI cases had a more westerly component of motion and were intensifying more during the preceding 12 h than the non-RI cases. No significant differences were found between the translational speeds of the RI and non-RI cases.
- The RI cases were farther from their maximum potential intensity and developed in regions of warmer water and higher lower-tropospheric relative humidity than the non-RI cases. Also, the RI cases were in regions of lower vertical shear and more easterly upper-tropospheric flow than the non-RI cases. Interestingly, RI was more likely to occur for systems that were in an environment where forcing from upper-level troughs or cold lows was weaker than average.
- A simple technique for estimating the probability of RI was developed. This technique compares the magnitudes of five predictors (previous 12-h intensity change, sea surface temperature, low-level relative humidity, vertical shear, and the difference between the current intensity and the maximum potential TC intensity) to previously determined RI thresholds. It was employed in real time during the 2001 Atlantic hurricane season for the first time.

While results from the first-year attempts to estimate the probability of RI are encouraging, future work will focus on investigating whether new predictors such as ocean heat content and GOES infrared imagery can be employed to improve the probability of RI estimates. Also, the possibility of employing more sophisticated statistical techniques (e.g., neural network) for estimating the probability of RI will be explored. The results of these efforts will be reported on in the near future.

Acknowledgments. We thank Drs. Sim Aberson and Chris Landsea and two anonymous reviewers for their constructive reviews of an earlier version of this man-

uscript. We also thank Drs. Lixion Avila and Richard Pasch, and James Franklin of the National Hurricane Center for their helpful suggestions and encouragement during the course of this study. Michael Black and Robert Black of HRD assisted with some of the graphics, and Robert Kohler, William Barry, and Joseph Griffin of HRD provided computer support. This research was partially funded by the Joint Hurricane Testbed (JHT) administered by the United States Weather Research Program (USWRP).

REFERENCES

Aberson, S., and M. DeMaria, 1994: Verification of a nested barotropic hurricane track forecast model (VICBAR). *Mon. Wea. Rev.*, **122,** 2804–2815.

Baik, J.-J., and H.-S. Hwang, 1998: Tropical cyclone intensity prediction using regression method and neural network. *J. Meteor. Soc. Japan*, **76,** 711–717.

Bender, M. A., and I. Ginis, 2000: Real-case simulations of hurricane–ocean interaction using a high-resolution coupled model: Effects on hurricane intensity. *Mon. Wea. Rev.*, **128,** 917–943.

——, ——, and Y. Kurihara, 1993: Numerical simulations of tropical cyclone–ocean interaction with a high-resolution coupled model. *J. Geophys. Res.*, **98,** 23 245–23 263.

Black, P. G., 1983: Ocean temperature changes induced by tropical cyclones. Ph.D. dissertation, The Pennsylvania State University, 278 pp. [Available from The Pennsylvania State University, University Park, PA 16802.]

Bosart, L. F., C. S. Velden, W. E. Bracken, J. Molinari, and P. G. Black, 2000: Environmental influences on the rapid intensification of Hurricane Opal (1995) over the Gulf of Mexico. *Mon. Wea. Rev.*, **128,** 322–352.

Byers, H. R., 1944: *General Meteorology.* McGraw-Hill, 645 pp.

Caplan, P., J. Derber, W. Gemmill, S.-Y. Hong, H.-L. Pan, and D. Parrish, 1997: Changes to the 1995 NCEP operational Medium-Range Forecast model analysis–forecast system. *Wea. Forecasting*, **12,** 581–594.

Cione, J. J., and E. W. Uhlhorn, 2003: Sea surface temperature variability in hurricanes: Implications with respect to intensity change. *Mon. Wea. Rev.*, **131,** 1783–1796.

DeMaria, M., 1996: The effect of vertical shear on tropical cyclone intensity change. *J. Atmos. Sci.*, **53,** 2076–2087.

——, and J. Kaplan, 1994a: A Statistical Hurricane Intensity Prediction Scheme (SHIPS) for the Atlantic basin. *Wea. Forecasting*, **9,** 209–220.

——, and ——, 1994b: Sea surface temperature and the maximum intensity of Atlantic tropical cyclones. *J. Climate*, **7,** 1324–1334.

——, and ——, 1999: An updated statistical hurricane intensity prediction scheme for the Atlantic and eastern North Pacific basins. *Wea. Forecasting*, **14,** 326–337.

——, J.-J Baik, and J. Kaplan, 1993: Upper-level eddy angular momentum flux and tropical cyclone intensity change. *J. Atmos. Sci.*, **50,** 1133–1147.

——, R. M. Zehr, J. P. Kossin, and J. A. Knaff, 2002: The use of GOES imagery in statistical hurricane intensity prediction. Preprints, *25th Conf. on Hurricanes and Tropical Meteorology*, San Diego, CA, Amer. Meteor. Soc., 120–121.

Dowdy, S., and S. Wearden, 1991: *Statistics for Research.* 2d ed. Wiley-Interscience, 555 pp.

Dunion, J. P., and C. S. Velden, 2002: Satellite applications for tropical wave/tropical cyclone tracking. Preprints, *25th Conf. on Hurricanes and Tropical Meteorology*, San Diego, CA, Amer. Meteor. Soc., 132–133.

Emanuel, K. A., 1986: An air–sea interaction theory for tropical cyclones. Part I: Steady-state maintenance. *J. Atmos. Sci.*, **43,** 585–604.

——, 1988: The maximum intensity of hurricanes. *J. Atmos. Sci.*, **45,** 1143–1155.

——, 2000: Thermodynamic control of hurricane intensity. *Nature*, **401,** 665–669.

Fitzpatrick, P. J., 1997: Understanding and forecasting tropical cyclone intensity change with the Typhoon Intensity Prediction Scheme (TIPS). *Wea. Forecasting*, **12,** 826–846.

——, J. A. Knaff, C. W. Landsea, and S. V. Finley, 1995: Documentation of a systematic bias in the Aviation Model's forecast of the Atlantic tropical upper-tropospheric trough: Implications for tropical cyclone forecasting. *Wea. Forecasting*, **10,** 433–446.

Frank, W. M., and E. A. Ritchie, 1999: Effects of environmental flow upon tropical cyclone structure. *Mon. Wea. Rev.*, **127,** 2044–2061.

——, and ——, 2001: Effects of vertical wind shear on the intensity and structure of numerically simulated hurricanes. *Mon. Wea. Rev.*, **129,** 2249–2269.

——, and ——, 2002: Tropical cyclones in complex vertical shears, 2002. Preprints, *25th Conf. on Hurricanes and Tropical Meteorology*, San Diego, CA, Amer. Meteor. Soc., 315–316.

Gray, W. M., 1968: Global view of the origin of tropical disturbances and storms. *Mon. Wea. Rev.*, **96,** 669–700.

Gross, J. M., 2001: North Atlantic and east Pacific track and intensity verification for 2000. *Minutes of the 55th Interdepartmental Hurricane Conf.*, Miami, FL, Office of the Federal Coordinator for Meteorological Services and Supporting Research, NOAA, B12–B15. [Available from Federal Coordinator for Meteorological Services and Supporting Research, 6101 Executive Blvd., Ste. 900, Rockville, MD 20852.]

Hanley, D., J. Molinari, and D. Keyser, 2001: A composite study of the interactions between tropical cyclones and upper-tropospheric troughs. *Mon. Wea. Rev.*, **129,** 2570–2584.

Holliday, C. R., and A. H. Thompson, 1979: Climatological characteristics of rapidly intensifying typhoons. *Mon. Wea. Rev.*, **107,** 1022–1034.

Hong, X., S. W. Chang, S. Raman, L. K. Shay, and R. Hodur, 2000: The interaction between Hurricane Opal (1995) and a warm core ring in the Gulf of Mexico. *Mon. Wea. Rev.*, **128,** 1347–1365.

Jarvinen, B. R., C. J. Neumann, and M. A. S. Davis, 1984: A tropical cyclone data tape for the North Atlantic basin, 1886–1983: Contents, limitations, and uses. NOAA Tech. Memo. NWS NHC 22, Miami, FL, 21 pp. [Available from National Technical Information Service, 5285 Port Royal Rod., Springfield, VA 22151.]

Lamb, P. J., 1984: On the mixed-layer climatology of the north and tropical Atlantic. *Tellus*, **36A,** 292–305.

Landsea, C. W., and Coauthors, 2003: The Atlantic hurricane database reanalysis project: Documentation for the 1851–1910 alterations and additions to the HURDAT database. *Hurricanes and Typhoons: Past, Present and Future*, R. J. Murnane and K. B. Liu, Eds., Columbia University Press, in press.

Lawrence, M. B., B. M. Mayfield, L. A. Avila, R. J. Pasch, and E. N. Rappaport, 1998: Atlantic hurricane season of 1995. *Mon. Wea. Rev.*, **126,** 1124–1151.

——, L. A. Avila, J. L. Beven, J. L. Franklin, J. L. Guiney, and R. J. Pasch, 2001: Atlantic hurricane season of 1999. *Mon. Wea. Rev.*, **129,** 3057–3084.

Levitus, S., 1982: *Climatological Atlas of the World Ocean.* NOAA Prof. Paper 13, 173 pp. [Available from U.S. Government Printing Office, Washington, DC 20402.]

Malkus, J. S., and H. Riehl, 1960: On the dynamics and energy transformations in steady-state hurricanes. *Tellus*, **12,** 1–20.

Merrill, R. T., 1988: Environmental influences on hurricane intensification. *J. Atmos. Sci.*, **45,** 1678–1687.

Miller, B. I., 1958: On the maximum intensity of hurricanes. *J. Meteor.*, **15,** 184–195.

Molinari, J., and D. Vollaro, 1989: External influences on hurricane intensity. Part I: Outflow-layer eddy angular momentum fluxes. *J. Atmos. Sci.*, **46,** 1093–1105.

——, and ——, 1990: External influences on hurricane intensity. Part

II: Vertical structure and response of the hurricane vortex. *J. Atmos. Sci.,* **47,** 1902–1918.

——, S. Skubis, and D. Vollaro, 1995: External influences on hurricane intensity. Part III: Potential vorticity structure. *J. Atmos. Sci.,* **52,** 3593–3606.

Moller, D. J., and M. T. Montgomery, 2000: Tropical cyclone evolution via potential vorticity anomalies in a three-dimensional balance model. *J. Atmos. Sci.,* **57,** 3366–3387.

Montgomery, M. T., and R. J. Kallenbach, 1997: A theory for vortex Rossby waves and its application to spiral bands and intensity changes in hurricanes. *Quart. J. Roy. Meteor. Soc.,* **123,** 435–465.

Neumann, C. J., B. R. Jarvinen, C. J. McAdie, and G. R. Hammer, 1999: Tropical cyclones of the North Atlantic Ocean, 1871–1998. Historical Climatology Series, No. 6-2, National Climatic Data Center, 206 pp. [Available from National Climatic Data Center, 151 Patton Ave., Asheville, NC 28801.]

Persing, J., M. T. Montgomery, and R. E. Tuleya, 2002: Environmental interactions in the GFDL hurricane model for Hurricane Opal. *Mon. Wea. Rev.,* **130,** 298–317.

Pfeffer, R. L., 1958: Concerning the mechanics of hurricanes. *J. Meteor.,* **15,** 113–120.

——, and M. Challa, 1981: A numerical study of the role of eddy fluxes of momentum in the development of Atlantic hurricanes. *J. Atmos. Sci.,* **38,** 2393–2398.

Reynolds, R. W., and T. M. Smith, 1993: An improved real-time global sea surface temperature analysis. *J. Climate,* **6,** 114–119.

Sadler, J. C., M. A. Lander, A. M. Hori, and L. K. Oda, 1987: *Indian Ocean and Atlantic Ocean.* Vol. 1, *Tropical Marine Climatic Atlas.* [Available from Department of Meteorology, University of Hawaii, Honolulu, HI 96822.]

Saffir, H. S., 1973: Hurricane wind and storm surge. *Military Eng.,* **423,** 4–5.

Schade, L. R., and K. A. Emanuel, 1999: The ocean's effect on the intensity of tropical cyclones: Results from a simple coupled atmosphere–ocean model. *J. Atmos. Sci.,* **56,** 642–651.

Shay, L. K., G. J. Goni, and P. G. Black, 2000: Effects of a warm oceanic feature on Hurricane Opal. *Mon. Wea. Rev.,* **128,** 1366–1383.

Simpson, R. H., 1974: The hurricane disaster potential scale. *Weatherwise,* **27,** 169, 186.

Sutyrin, G. G., and A. P. Khain, 1979: Interaction of the ocean and the atmosphere in the area of moving tropical cyclone. *Dokl. Akad. Nauk. SSR,* **249,** 467–470.

Willoughby, H. E., J. A. Clos, and M. G. Shoreibah, 1982: Concentric eyewalls, secondary wind maxima, and the evolution of the hurricane vortex. *J. Atmos. Sci.,* **39,** 395–411.